Cluster Formation of Transmembrane Proteins Due to Hydrophobic Mismatching

Ulrich Schmidt, Gernot Guigas, and Matthias Weiss

Cellular Biophysics Group (BIOMS), German Cancer Research Center, Im Neuenheimer Feld 280, D-69120 Heidelberg, Germany

(Received 26 March 2008; published 19 September 2008)

Membranes are the defining envelopes of living cells. At this boundary a multitude of transmembrane proteins mediate signal and mass transfer between cells and their environment. Clustering of these proteins is a frequent and often vital phenomenon that relies at least in part on membrane-mediated interactions. Indeed, the mismatch between proteins' hydrophobic transmembrane domains and the surrounding lipid bilayer has been predicted to facilitate clustering, yet unequivocal quantitative data in support of these predictions have been lacking. Here, we have used coarse-grained membrane simulations to thoroughly address the clustering of transmembrane proteins in detail. Our results emphasize the universal nature of membrane-mediated attraction which relaxes the need for a plethora of fine-tuned interactions between membrane proteins.

DOI: 10.1103/PhysRevLett.101.128104 PACS numbers: 87.15.kt, 87.16.A−, 87.16.D−

Being more than passive envelopes, biomembranes mediate signal and mass transfer from the environment to the cell's interior via a multitude of transmembrane proteins [1]. Membrane proteins often cluster to perform their function, e.g., to participate in protein sorting during secretion processes [2]. While specific bimolecular binding events are traditionally made responsible for the formation of protein clusters, several lines of evidence indicate that unspecific, membrane-mediated interactions also play a major role in these events [3], thus relaxing the need for a multitude of fine-tuned interactions.

In the context of membrane-mediated interactions the effects of a ''hydrophobic mismatch'' has been of particular interest (see, e.g., [4] for review): When the hydrophobic transmembrane domain of a protein does not match the thickness of the lipid bilayer's hydrophobic core, clustering of proteins has been predicted [5], e.g., within the framework of the ''mattress model'' [6], within a phenomenological mean-field elasticity approach [7], and within a detailed model based on capillary forces [8].

While hydrophobic-mismatch driven clustering has been studied extensively by mean-field theories [4], supporting experimental studies [9] have remained rare and equivocal in highlighting the pure effects of hydrophobic mismatching. In particular, it has remained unclear whether the mean-field predictions are actually capable of describing the natural situation in which the lipid bilayer is not a homogenous two-dimensional fluid but rather is composed of individual lipids with similar dimensions as the embedded proteins. Since quantitative experiments are challenging in several aspects, computer simulations lend themselves as a powerful alternative to address this issue.

To study the local change of the lipid environment around proteins with varying hydrophobic mismatch and the effective attraction that drives clustering, we have used dissipative particle dynamics (DPD). In accordance with standard DPD models [10,11], we have imposed a linear repulsive force $\mathbf{F}_{ij}^{C} = a_{ij}(1 - r_{ij}/r_0)\hat{\mathbf{r}}_{ij}$ between any two beads i, j having a distance $r_{ij} = |\mathbf{r}_{ij}| = |\mathbf{r}_i - \mathbf{r}_j| \leq r_0$ (with $\hat{\mathbf{r}}_{ij} = \mathbf{r}_{ij}/r_{ij}$ denoting the corresponding unit vector). The degree of hydrophobicity was tuned via the interaction energies a_{ij} while bonds within lipids and proteins were modeled via a harmonic potential $U(\mathbf{r}_i, \mathbf{r}_{i+1}) = k(r_{i,i+1} - l_0)^2/2$ between the respective beads. Lipids and proteins were given an additional bending stiffness via the potential $V(\mathbf{r}_{i-1}, \mathbf{r}_i, \mathbf{r}_{i+1}) = \kappa[1 - \cos(\phi)]$ with $\cos\phi = \hat{\mathbf{r}}_{i-1,i} \cdot \hat{\mathbf{r}}_{i,i+1}$. For the thermostat, dissipative and random forces were given by $\mathbf{F}_{ij}^{D} = -\gamma_{ij}(1 - r_{ij}/r_0)^2(\hat{\mathbf{r}}_{ij} \cdot \mathbf{v}_{ij})\hat{\mathbf{r}}_{ij}$ and $\mathbf{F}_{ij}^{R} = \sigma_{ij}(1 - r_{ij}/r_0)\zeta_{ij}\hat{\mathbf{r}}_{ij}$, respectively, when $r_{ij} \leq r_0$. Here, $\mathbf{v}_{ij} = \mathbf{v}_i - \mathbf{v}_j$ denotes the relative velocity between the particles i, j while ζ_{ij} is a random variable with $\langle\zeta_{ij}\rangle = 0$ and $\langle\zeta_{ij}\zeta_{kl}\rangle = \delta_{ik}\delta_{jl}$. The parameters γ_{ij} and σ_{ij} are related via the fluctuation-dissipation theorem $\sigma_{ij}^2 = 2\gamma_{ij}k_BT$ [11].

The interaction cutoff r_0, all bead masses, and the thermostat temperature k_BT were set to unity. In accordance with [12], we have chosen $\sigma_{ij} = 3$, $\gamma_{ij} = 9/2$, $k = 100k_BT/r_0^2$, $l_0 = 0.45r_0$, $\kappa = 20k_BT$, $a_{HT} = a_{WT} = 200k_BT$, and $a_{WW} = a_{HH} = a_{TT} = a_{WH} = 25k_BT$ (indices W, H, T denoting water, lipid head, lipid tail bead, respectively). Lipids were modeled as a linear chain (HT_3), while proteins were modeled as filled hexagons of HT_nH chains (cf. Fig. 1). We have integrated the equations of motion with a velocity Verlet scheme [13] (time increment $\Delta t = 0.01$) using periodic boundary conditions. To achieve a tensionless membrane, we first equilibrated the system for 5×10^4 steps with a barostat [14] and then fixed the length of the simulation box for the remaining 10^6 simulation steps. The intrinsic DPD units may be converted to SI units ($r_0 \equiv 1$ nm, $\Delta t \equiv 80$ ps) by gauging the membrane thickness and the lipids' diffusion coefficient [15].

We first monitored the steady-state membrane thickness in the vicinity of a single protein embedded in a membrane of linear size $L = 20r_0$. Varying the number n of hydrophobic layers in the core of the hexagonal protein/inclusion,

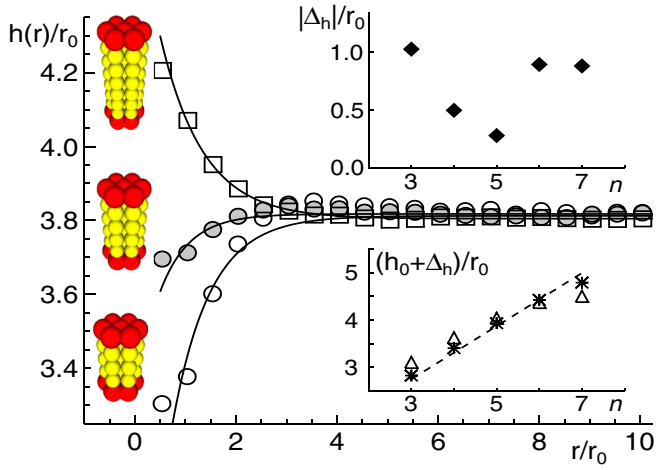

FIG. 1 (color online). The numerically determined radial bilayer thickness $h(r)$ is well described by an exponential profile (full lines) for negative (open circles), almost vanishing (filled circles), and positive (open squares) hydrophobic mismatches. Insets on the left show the respective inclusions with $n = 3, 4, 6$ transmembrane layers. Inset, top: The mismatch Δ_h with respect to the unperturbed bilayer thickness $h_0 \approx 3.8r_0$ is smallest for $n = 5$. For $n > 6$, the bilayer cannot be stretched any further and the inclusion tilts [cf. Fig. 2(a)]. Inset, bottom: The maximum thickness of the membrane $h_0 + \Delta_h$ at the inclusion grows linearly with the inclusion's number of hydrophobic layers, n.

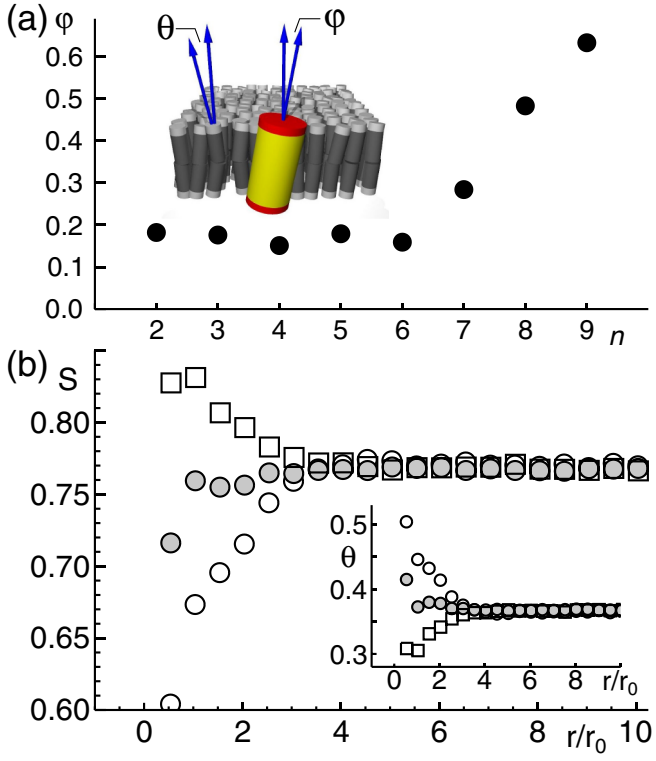

FIG. 2 (color online). (a) For a strong positive hydrophobic mismatch ($n \geq 7$), the inclusion starts to tilt with respect to the bilayer normal (angle φ). (b) The local lipid orientation as determined via the order parameter S (cf. main text) clearly deviates from the value for an unperturbed lipid bilayer in the vicinity of the inclusion. For small distances r, a strong reduction or increase in S is seen for negative ($n = 3$, open circles) or positive ($n = 6$, open squares) hydrophobic mismatches, respectively. The deviations are considerably smaller for $n = 4$ (filled circles). Inset: The average angle θ between the lipids and the surface normal strongly deviates from the unperturbed value $\theta \approx 0.36$ far away from the inclusion.

i.e., varying the hydrophobic mismatch, we observed in all cases that the bilayer thickness around the protein showed an exponential decay $h(r) = h_0 + \Delta_h e^{-r/\lambda}$ (Fig. 1) towards the bilayer thickness without protein ($h_0 \approx 3.8r_0$), in agreement with theoretical predictions [7]. Using $h(r) \sim K_0(r/l_c)$ [8] as an alternative expression (K_0 denotes the modified Bessel function of order zero) yielded a significantly less good fit. As expected, the maximum membrane thickness $h_0 + \Delta_h$ obtained from the fitting with an exponential varied linearly with the number n of hydrophobic layers in the inclusion (Fig. 1, lower inset). For $n = 5$, the thickening of the bilayer $\Delta_h$was smallest (Fig. 1, upper inset); i.e., the hydrophobic mismatch almost vanished. While Δ_h increased monotonically for $n \leq 5$, the thickening of the bilayer remained constant for $n > 6$. This behavior can be understood when inspecting the orientation angle φ of the inclusion with respect to the bilayer normal [Fig. 2(a)]: For $n > 6$ it becomes energetically favorable to tilt the inclusion rather than to further stretch the bilayer. In the remainder we hence concentrate on $n \leq 6$.

We next inspected the orientation angle $\theta(r)$ of lipids in the inclusion's surrounding (Fig. 2). The average tilt angle in an unperturbed membrane may be estimated as $\langle\theta\rangle = \text{atan}\sqrt{A/(\pi\ell^2)} \approx 0.36$ from a lipid's cylindrical envelope, i.e., via the average area per lipid ($A \approx 1.43/r_0^2$) and the typical lipid length ($\ell = 1.8r_0$). Indeed, we see a good agreement with this estimate far away from the inclusion [Fig. 2(b), inset] while $\theta(r)$ significantly deviates from this value near to the inclusion. To describe this local change in lipid orientation it is most convenient to use the orientational order parameter $S(r) = \langle[3\cos^2(\theta) - 1]/2\rangle$. As expected from the angles θ, the lipids' orientation was very variable far away from the inclusion ($S \approx 0.77$). For a positive hydrophobic mismatch, S increased significantly near to the inclusion (Fig. 2), highlighting a local ordering of the lipids parallel to the surface normal ($S \rightarrow 1$). In contrast, a negative hydrophobic mismatch had the opposite effect (lower S). Inward-bending lipids tried to cover the hydrophobic core of the bilayer that cannot be in direct contact with the hydrophobic portion of the inclusion. Our results thus indicate that lipids in an annulus around an inclusion have a lower entropy due to their constrained configuration as compared to their mates in an unperturbed bilayer. This decrease in entropy may be expected to drive a clustering of inclusions, similar to the formation of micelles in water-oil mixtures.

To probe this prediction, we next embedded two inclusions into a bilayer ($L = 20r_0$). By monitoring the force components along the unit vector pointing from one pro-

tein to the other, we determined via integration the pair potential $U(r)$ that the proteins experienced [Fig. 3(a)]. For all proteins we observed a minimum in $U(r)$ when the proteins touched ($r = 0$) while for increasing distances ($r \approx r_0/2$) a high potential barrier emerged that was followed by 2–3 lower peaks. The potential maximum depended on the degree of hydrophobic mismatch, i.e., on n. Beyond $r \approx 3r_0$, the potential became essentially flat and the inclusions behaved as free and independent particles. The envelopes of $U(r)$ agree in gross terms with the theoretical predictions of [7], but not with the capillary interaction energy derived in [8]. We also did not observe the predicted stronger attraction for a negative hydrophobic mismatch as compared to a positive mismatch with similar Δ_h [8]. The fine structure in $U(r)$ as compared to the mean-field prediction [7] most likely is due to the discreteness of the membrane.

Interestingly, we observed a transient dimer formation even for an almost vanishing hydrophobic mismatch ($n =$ 5). It is tempting to speculate that in this case not the (fairly small) hydrophobic mismatch but rather the local geometric constraints of the surrounding lipids contribute to the effective attraction.

We next extracted from the simulations the average time τ_n for which the two proteins with a transmembrane portion n stayed within a distance $r \leq 3r_0$. For the smallest hydrophobic mismatch ($n = 5$) we obtained a dimer lifetime $\tau_5 \approx 183$ which corresponds to a real time of about 2 μs. For increasing hydrophobic mismatches, we observed a strong increase in the relative dimer lifetimes [Fig. 3(b)]. Indeed, for $n = 7$, i.e., a strong positive hydrophobic mismatch, the dimer lifetime increased more than 30-fold. For comparison we calculated from $U(r)$ the relative increase of the corresponding mean-first passage time t_n, describing the transition from the bound state ($r = 0$) to the free state ($r = 3r_0$). In agreement with our results on the dimer lifetimes τ_n, we observed a strong increase of t_n for increasing hydrophobic mismatches [Fig. 3(b)]. Thus, we can conclude that already dimers can be fairly stable entities with lifetimes up to $\sim$100 μs.

To go beyond the formation of dimers, we next investigated the formation of clusters using 30 proteins in a membrane ($L = 50r_0$). As can be seen from Fig. 4, a positive ($n = 6$) hydrophobic mismatch (and also negative mismatches; data not shown) gave rise to a strong clustering while a vanishing mismatch ($n = 5$) resulted in the transient formation of dimers only. Thus, in agreement with theoretical predictions and our above results, hydrophobic mismatching indeed drives cluster formation of membrane proteins.

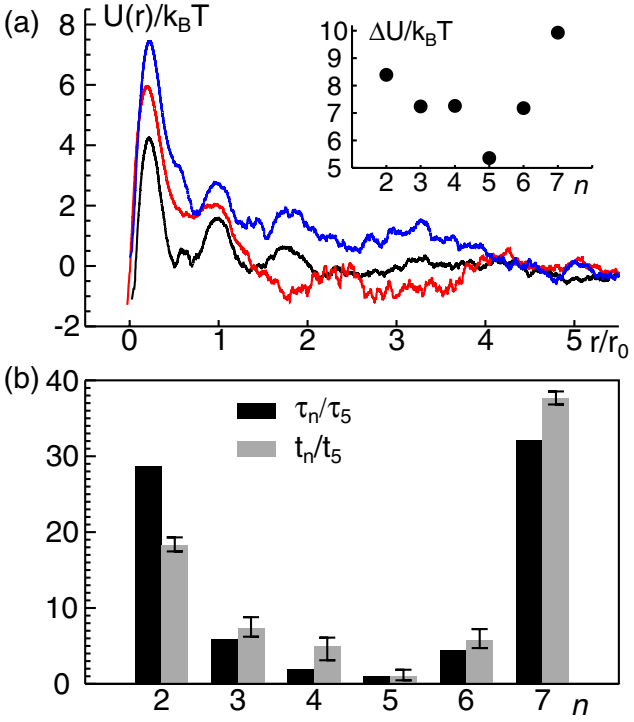

FIG. 3 (color online). (a) The mean pair potential between two inclusions with $n = 3, 5, 6$ (middle, lower, upper), as extracted from the simulations, shows a minimum for vanishing distance followed by a pronounced peak and several smaller peaks. Overcoming the potential barrier, say from $r = 0$ to $r = 3r_0$, determines the finite lifetimes of dimers. Inset: The energy difference $\Delta U = \max(U) - U(0)$ already indicates that dimers with $n \neq 5$ have an increased lifetime. (b) The mean dimer lifetimes τ_n as extracted from the simulations agree well with the predicted mean-first passage times t_n derived from the potentials $U(r)$. Error bars show the variation of t_n when considering an escape to distances $2r_0, \ldots, 4r_0$. All times are expressed with respect to τ_5 and t_5 ($n = 5$ had the smallest hydrophobic mismatch), respectively.

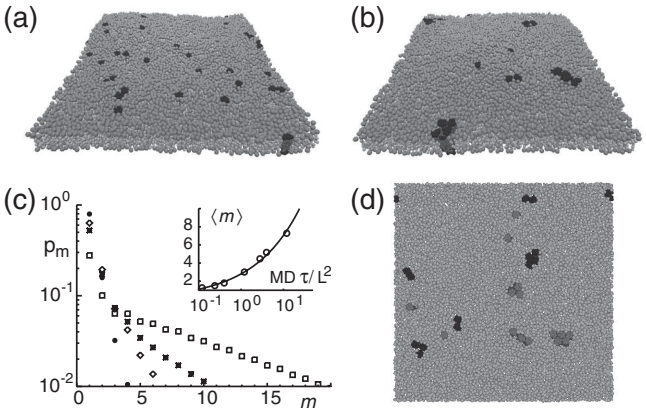

FIG. 4. Simulation snapshots after $\sim 10^6$ time steps for (a) vanishing ($n = 5$) and (b) positive ($n = 6$) hydrophobic mismatch. For $n = 5$ mainly dimers are observed while also larger clusters emerged for $n = 6$. (c) The cluster size distribution [Eq. (1)] for $DM\tau/L^2 = 0.12$, 0.4, 1.2, 12 (circles, diamonds, asterisks, squares) highlights the occurrence of larger aggregates for increasing hydrophobic mismatches (i.e., dimer lifetimes). Inset: The mean cluster size increases approximately like $\langle m \rangle \sim \tau^{0.4}$. (d) Using equal amounts of two different inclusions (dark gray: $n = 3$, light gray: $n = 6$) yields a demixing of proteins according to their hydrophobic mismatch (top view).

Since estimating the lifetimes of larger clusters and/or determining the distribution of cluster sizes via simulations is not feasible due to the prohibitively large computation times, we have considered the following model to estimate the number of m-clusters p_m given that the system consists of M pointlike proteins:

$$\frac{dp_m}{dt} = J_m + \frac{R}{2}\sum_{i=1}^{m-1} p_i p_{m-i}(1+\delta_{i,m-i}) - R\sum_{i=1}^{M-m} p_m p_i(1+\delta_{i,m}). \quad (1)$$

The first term describes the loss of single proteins from a cluster's circumference, i.e. $J_m = \gamma(\sqrt{m+1}\,p_{m+1} - \sqrt{m}\,p_m)$ $(1 < m < M)$, $J_M = -\gamma\sqrt{M}\,p_M$, and $J_1 = \gamma\sqrt{8}p_2 + \gamma\sum_{k=3}^{M}\sqrt{k}\,p_k$. The evaporation rate γ may be identified with the inverse dimer lifetime ($\gamma = 1/\tau$). The two remaining terms in Eq. (1) describe the gain or loss of m clusters due to the diffusively driven aggregation of two clusters. Bearing in mind that the diffusion coefficient D hardly varies with size for small membrane inclusions [16], the rate R may be identified with the inverse diffusive search time on the membrane of length L, i.e. $R = D/L^2$. Please note that $\sum_{m=1}^{M} m p_m = M$ is conserved under the dynamics while $\sum_{m=1}^{M} p_m$ is not. The steady-state distribution for varying values of the ratio $MD\tau/L^2$, i.e., for various hydrophobic mismatches, are shown in Fig. 4(c). Using the numerically obtained values for τ and D, the model predicts that clusters up to 10 mers are likely to exist for large hydrophobic mismatches. This is also underlined by the growth of the mean cluster size $\langle m\rangle$ for increasing $MD\tau/L^2$. In addition, a large amount of monomers and dimers is expected. Given the simplicity of Eq. (1) and the numerical observation that large clusters appear even more stable than dimers, Eq. (1) can be expected to actually underestimate the mean cluster size by overestimating the number of free monomers. Indeed, our simulations support this notion, albeit with poor statistics [cf. Fig. 4(b)]. Nevertheless, Eq. (1) is a valuable tool to obtain a lower bound for the mean cluster size.

Going beyond the case of a pure ensemble, we also considered two species of membrane proteins having different hydrophobic mismatches. In particular, when using equal amounts of proteins with $n = 3$ and $n = 6$, we observed a clear separation of the two species [Fig. 4(d)]. While this strong segregation may not come unexpected for the case of a negative and a positive hydrophobic mismatch, we observed a similar demixing even when both proteins had similar hydrophobic mismatches (e.g., $n = 6, 7$). A more detailed investigation of this demixing is currently in progress and will be presented elsewhere.

In conclusion, we have unequivocally shown that membrane proteins can cluster due to hydrophobic mismatching with their lipid environment. The membrane-mediated clustering is due to an effective attractive pair potential between membrane inclusions with a rich fine structure. Based on simple kinetic considerations and on the observation of rapidly increasing dimer lifetimes when the hydrophobic mismatch is enhanced, it is highly likely that bigger clusters have large enough lifetimes to play a major role in the biological context. Moreover, a membrane-mediated nonspecific attraction may facilitate specific interactions between transmembrane proteins by increasing the residence time in the bimolecular reaction zone. Bearing in mind the universal method of clustering and the observed demixing of proteins we further hypothesize that living cells may use membrane-mediated interactions to support protein sorting in the secretory pathway [17].

This work was supported by the Institute for Modeling and Simulation in the Biosciences (BIOMS) in Heidelberg. U. S. was funded by the FORSYS initiative of the German Federal Ministery of Education and Research.

[1] B. Alberts *et al.*, *Molecular Biology of the Cell* (Garland Publishing, New York, 1994), 3rd ed.
[2] M. Bagnat *et al.*, Proc. Natl. Acad. Sci. U.S.A. **97**, 3254 (2000).
[3] R. Bruinsma and P. Pincus, Curr. Opin. Solid State Mater. Sci. **1**, 401 (1996); K. Simons and E. Ikonen, Nature (London) **387**, 569 (1997); M. Edidin, Annu. Rev. Biophys. Biomol. Struct. **32**, 257 (2003).
[4] M. Jensen and O. G. Mouritsen, Biochim. Biophys. Acta **1666**, 205 (2004).
[5] S. Marčelja, Biochim. Biophys. Acta **455**, 1 (1976).
[6] O. G. Mouritsen and M. Bloom, Biophys. J. **46**, 141 (1984).
[7] N. Dan, P. Pincus, and S. A. Safran, Langmuir **9**, 2768 (1993); N. Dan, A. Berman, P. Pincus, and S. A. Safran, J. Phys. II (France) **4**, 1713 (1994).
[8] P. A. Kralchevsky, V. N. Paunov, N. D. Denkov, and K. Nagayama, J. Chem. Soc., Faraday Trans. **91**, 3415 (1995).
[9] B. Lewis and D. Engelman, J. Mol. Biol. **166**, 203 (1983); T. Harroun *et al.*, Biophys. J. **76**, 937 (1999).
[10] P. J. Hoogerbrugge and J. M. V. A. Koelman, Europhys. Lett. **19**, 155 (1992); R. D. Groot and P. B. Warren, J. Chem. Phys. **107**, 4423 (1997).
[11] P. Español and P. B. Warren, Europhys. Lett. **30**, 191 (1995).
[12] M. Laradji and P. B. S. Kumar, Phys. Rev. Lett. **93**, 198105 (2004).
[13] P. Nikunen, M. Karttunen, and I. Vattulainen, Comput. Phys. Commun. **153**, 407 (2003).
[14] A. F. Jakobsen, J. Chem. Phys. **122**, 124901 (2005).
[15] A. F. Jakobsen, O. G. Mouritsen, and M. Weiss, J. Phys. Condens. Matter **17**, S4015 (2005).
[16] P. G. Saffman and M. Delbrück, Proc. Natl. Acad. Sci. U.S.A. **72**, 3111 (1975).
[17] M. Bretscher and S. Munro, Science **261**, 1280 (1993).